Compensating Langmuir Probe Studies on the Production of High-Density Plasma in RF Transformer Coupled Discharge

Boonchoat Paosawatyanyong

A radio frequency (RF) transformer coupled plasma (TCP) reactor was designed and set up as a high-density plasma source. The system is powered by a 13.56-MHz 1000-W RF generator. The RF field was coupled into the plasma *via* an impedance matching network consisting of a tunable vacuum capacitor and planar induction coil. The experimental study to obtain the plasma parameters inside the system was conducted using the self-compensating Langmuir probe technique. Electron temperature during the discharge was found to be from 2.5 to 4 eV. Plasma density was found to be in the range of 2.2×10^{10} to 1.48×10^{12} cm^{-3}. The plasma potential of the TCP was between 12 to 20 V. An abrupt increase in the plasma density during mode transition of the TCP plasma was observed. On the other hand, neither an abrupt change in the electron temperature nor the plasma potential was observed during such mode transition.

Key words: RF plasma, Langmuir probe and plasma parameters.

Department of Physics, Faculty of Science, Chulalongkorn University, Bangkok 10330, Thailand.

** Correspondence to: e-mail: paosawat@sc.chula.ac.th*

การศึกษาพลาสมาความหนาแน่นสูงของระบบการให้กำเนิดพลาสมาจากหลักการควบแปลงคลื่นความถี่วิทยุ โดยการวัดลางมัวร์แบบชดเชยค่าภายในตนเอง

บุญโชติ เผ่าสวัสดิ์ยรรยง (2547)

วารสารวิจัยวิทยาศาสตร์ จุฬาลงกรณ์มหาวิทยาลัย **29(2)**

ระบบการให้กำเนิดพลาสมาจากหลักการควบแปลงคลื่นความถี่วิทยุ ได้ถูกออกแบบและจัดสร้างขึ้นเพื่อใช้เป็นแหล่งพลาสมาความหนาแน่นสูง ระบบนี้ใช้แหล่งกำเนิดคลื่นวิทยุความถี่ 13.56 เมกกะเฮิรตซ์ ขนาด 1000 วัตต์ ส่งผ่านคลื่นเข้าสู่วงจรกำทอนความขัด ที่ประกอบด้วยตัวจุสุญญากาศแบบปรับค่าได้ และขดลวดเหนี่ยวนำวางแบนชุดหนึ่ง การวัดค่าตัวแปรพลาสมาภายในระบบได้กระทำโดยใช้เทคนิคการวัดลางมัวร์แบบชดเชยค่าภายในตนเอง ค่าอุณหภูมิอิเล็กตรอนที่วัดได้อยู่ระหว่าง 2.5 ถึง 4 อิเล็กตรอนโวลท์ ค่าความหนาแน่นพลาสมาอยู่ระหว่าง $2.2x10^{10}$ ถึง $1.48x10^{12}$ ต่อลูกบาศก์เซนติเมตร ค่าศักย์พลาสมาที่วัดได้อยู่ระหว่าง 12 ถึง 20 โวลท์ ผลการวัดความหนาแน่นพลาสมาพบว่า มีการเพิ่มแบบก้าวกระโดดในระหว่างการเปลี่ยนโหมดของระบบในทางตรงข้ามกลับไม่พบว่ามีการเปลี่ยนแปลงแบบก้าวกระโดดของอุณหภูมิอิเล็กตรอน หรือค่าศักย์พลาสมา ในช่วงการเปลี่ยนโหมดดังกล่าวแต่อย่างไร

คำสำคัญ พลาสมาคลื่นความถี่วิทยุ หัววัดลางมัวร์ ตัวแปรพลาสมา

INTRODUCTION

The widespread application of low-temperature plasma devices in modern technology has stimulated an extensive research effort into the inductively coupled plasmas (ICPs) with a keen interest as a potential new source for low-pressure operations.[1] It has been reported that low-pressure ICPs have advantages such as high plasma density,[2] reduction in ion damage[3] and independently controllable ion energy.[4-6]

In order to obtain detailed knowledge of the properties that define the plasma in ICPs, many plasma parameters must be defined. Such parameters include electron temperature, electron/ion/plasma density, and the dominant species involved in the reaction chosen. In any plasma processing system, the energies, with or from of which the ions strike the sample surfaces, must also be known, and these often require the determination of the plasma potential. As in many other areas of work, no one diagnostic tool or technique can be used to adequately define all of the parameters. Several techniques such as electric or electrostatic probing, plasma oscillation measurement,[7] optical emission and laser spectroscopy[8,9] and recombination radiation analysis[10] have been used with some success.

Among such techniques, the use of electric probes is one of the earliest techniques for plasma parameter measurement. Basically, an electric probe is a small electrode, usually a metal wire, inserted inside the plasma. Essentially, the method is based upon the interpretation of the current collected by a probe in the plasma as a function of the voltage applied to the probe. When one inserts a probe into plasma, the plasma will be disturbed by the probe. Since the disturbance is localized in most cases, one can describe the local properties of plasma at the measurement region.

One of the most common electric probe techniques is the Langmuir method.[11] Although this method is mainly utilized in conventional DC discharges, the successful usage of Langmuir probe measurements in the radio frequency (RF) plasmas has also been reported by research groups.[5,7,12-14] Chatterton et. al.[5] report the application of self-compensating electrostatic Langmuir probes in order to reduce the RF field interference which leads to data discrepancy up to the first harmonic effect. In their work, by embedding two parallel LC loops and cylindrical compensating electrode as part of the probe tip close to the measurement region, the authors obtained reproducible data with good accuracy.

With fast evolving technology in the micro and nano scale semiconductor industry, the need by high precision plasma sources with a high aspect etching ratio has led to even more extensive studies in the designing and construction of RF plasma systems of high plasma density ($>10^{10}$ cm^{-3}) at low pressure ($<10^{-2}$ torr). Several research groups have reported source configurations and techniques such as hallow cathode microwave-ICP hybrid sources,[16] magnetron-ICP hybrid sources,[17] grid-biasing ICP[14] and pulsed-plasma ICP[18] achieving plasma density of up to $6x10^{11}$ cm^{-3} without the use of magnetic constrain fields and at relatively low pressure and low RF power (< 1kW). The literature also reports a relatively effective method of ICP excitation to be using a planar coil to couple the RF field through a dielectric into the plasma chamber. This is known as transformer coupled plasmas (TCPs).[14,19]

In this present work, a 13.56 MHz RF planar coil TCP system was designed and setup. The experimental study to obtain the plasma parameters inside the system was conducted using the self-compensating Langmuir probe technique. The electron

temperatures and the plasma densities of the TCP plasma produced under different conditions were compared to those reported by others.

EXPERIMENTATION

Experimental setup

The schematic diagram of the designed RF-TCP system is shown in Figure 1. The major components of the system are the reactor chamber, the RF generator, the impedance matching network, the gas and pressure handling components and the probe diagnostic system. In this work, the plasma source is powered by a 1000-Watts 13.56-MHz RF generator (Dressler model Cesar-1310) with an output impedance of 50 Ω.

The matching network used in the system was based on a LC resonant circuit which consists of a variable vacuum capacitor and a 6-8 turns planar coil with a maximum diameter of 120 mm as the inductor. The variable vacuum capacitor can be varied in the range of 80 pF to 1000 pF. The coupling circuit of the matching network is shown in Figure 2. The RF power is supplied to the load via a 7:1 step down transformer so that its effective output impedance is converted to approximately 1 Ω.

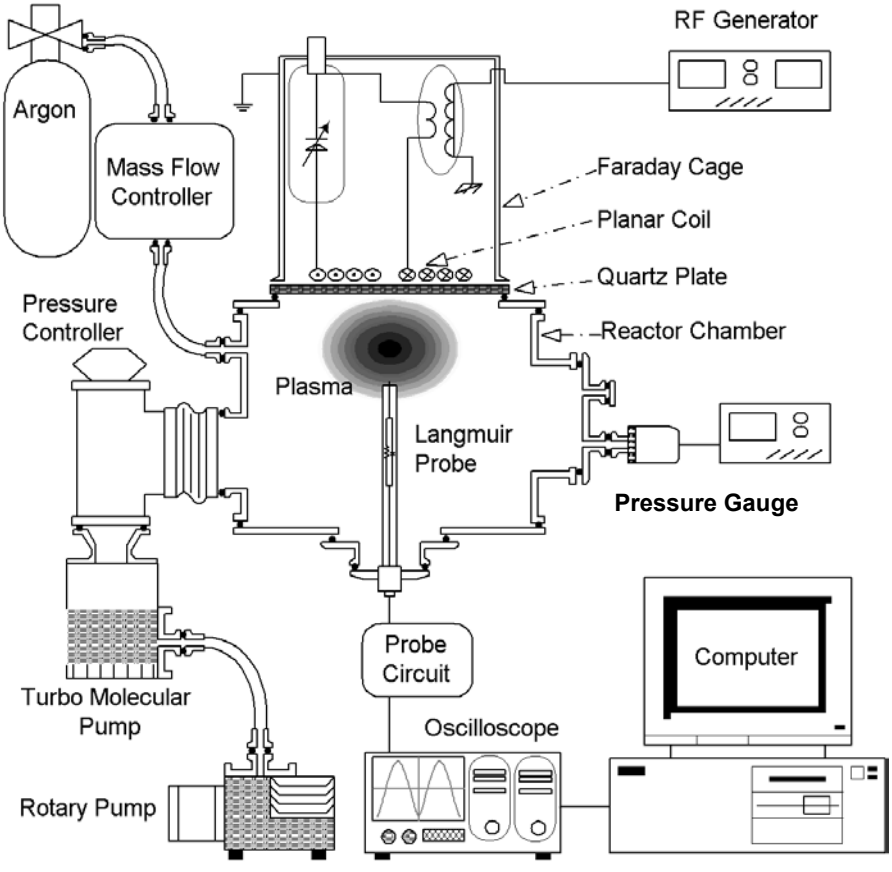

Figure 1. Schematic diagram of the RF-TCP system.

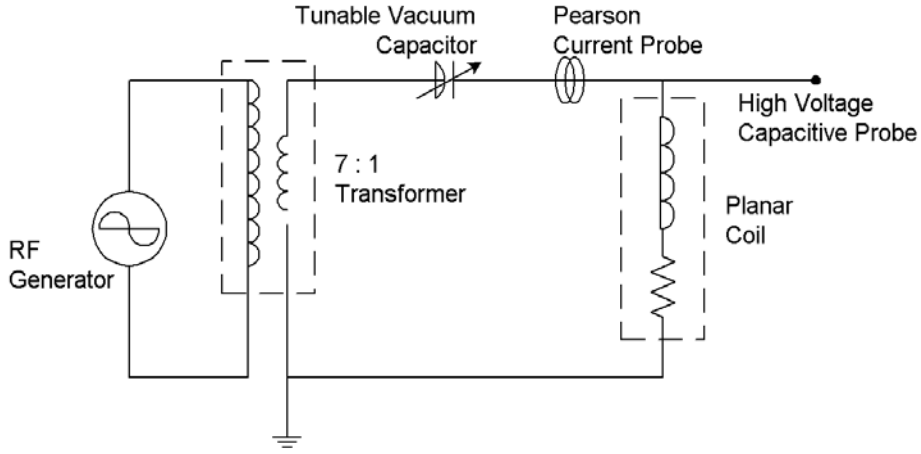

Figure 2. Coupling circuit of the Matching Network.

The matching network was placed inside a perforated aluminum cylinder, which acts as a Faraday cage in order to protect the electronic diagnostic instrument from the effects of stray RF fields. The planar coil current inside the cage is measured by a Pearson current probe, whereas the coil voltage is measured by high voltage capacitive probe.

The reactor chamber is made of stainless steel in a cylindrical form which is covered by stainless steel plates at the top and bottom flanges. The top plate has an opening which is covered by a quartz plate to isolate the vacuum. The planar coil is placed above the quartz plate.

The vacuum system consists of a turbo molecular pump backed by a rotary vane pump where a base pressure of 5.5×10^{-5} torr can be achieved. The pressure of the system is measured by a Penning type pressure gauge which was mounted at a port on the side flange of the chamber. During plasma operation, the operation gases entered the chamber via mass flow controllers (Dwyer GFC2100-series). An automated pressure controller (Edward 1800) was utilized to control the pressure inside the reactor chamber at the desired value.

Compensating Langmuir probe

The schematic diagram of the compensated Langmuir probe is shown in Figure 3. The probe's metal tip, which is exposed to the plasma, is made from nickel-chromium (Ni-Cr) alloy. The exposed tip has a diameter of 0.8 mm and the length of 2.2 mm. The part of the Ni-Cr wire which is not exposed to the plasma is covered by glass tube. In this RF compensated probe, a choke filter, consisting of a 0.34 μH inductor connecting in parallel with a 330pF capacitor, is placed in line with the probe wire to exert high impedance to RF noise. The values of the inductor (L) and capacitor (C) were obtained from equation (1).

$$f = \frac{1}{2\pi\sqrt{LC}} \qquad \ldots (1)$$

where, f is the applied RF frequency of 13.56 MHz.

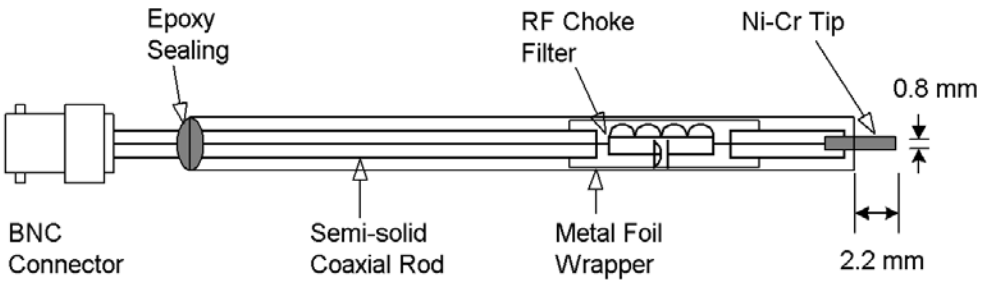

Figure 3. Schematic diagram of the RF compensating Langmuir probe.

The probe circuit shown in Figure 4 was used to obtain the I-V characteristics of the probe when interacting with the plasma. The probe current (I_p) and probe bias voltage (V_p) are monitored using a Tektronics digital oscilloscope. The probe was swept biased by a 250V peak-to-peak triangle-waveform voltage sweep amplifier. The sweep frequency was adjusted to minimize the discrepancy between the upper-sweep and lower-sweep turn of the measurement. Typical sweep rate used was between 0.5 - 10 V/μS. The Langmuir probe current was obtained by using a differential probe to measure the voltage drop across a 50 kΩ load. This across the load voltage was directly proportional to the probe current (I_p). Two RC low-pass filters, circuitry shown in Figure 4(b), were inserted in line between the detecting probes and the oscilloscope to further reduce the RF noise. The gain of the filter, $|G(f^*)|$ is defined in equation (2).

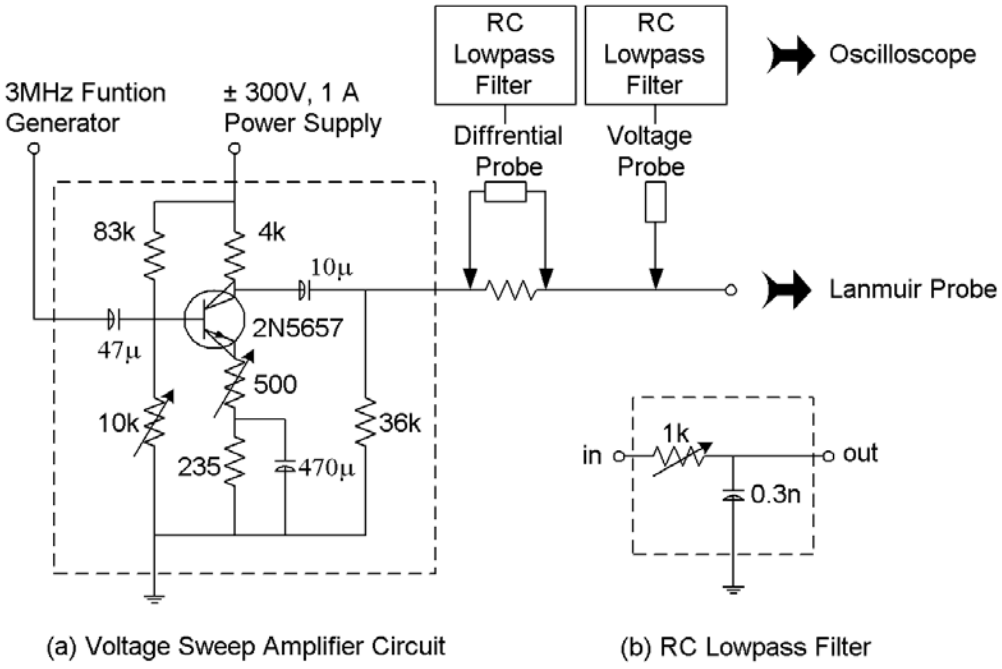

Figure 4. Schematic diagram of the circuit; (a) shows the Voltage Sweep Amplifier and (b) shows the RC Lowpass Filter.

$$|G(f^*)| = \frac{1}{\sqrt{1 + (2\pi f^* RC)^2}} \quad \ldots (2)$$

where, f^* is the RF noise frequency. From equation (2), $|G(f^*)|$ is zero as f^* approaches infinity. And vice versa, the magnitude of $|G(f^*)|$ approaches 1 as f^* approaches zero. In this experiment, a 10 kΩ variable resister and a 0.3 nF capacitor gave good results in suppressing the RF noise (f^*).

The typical I-V plot for the compensating Langmuir probe inside the TCP is shown in Figure 5(a).

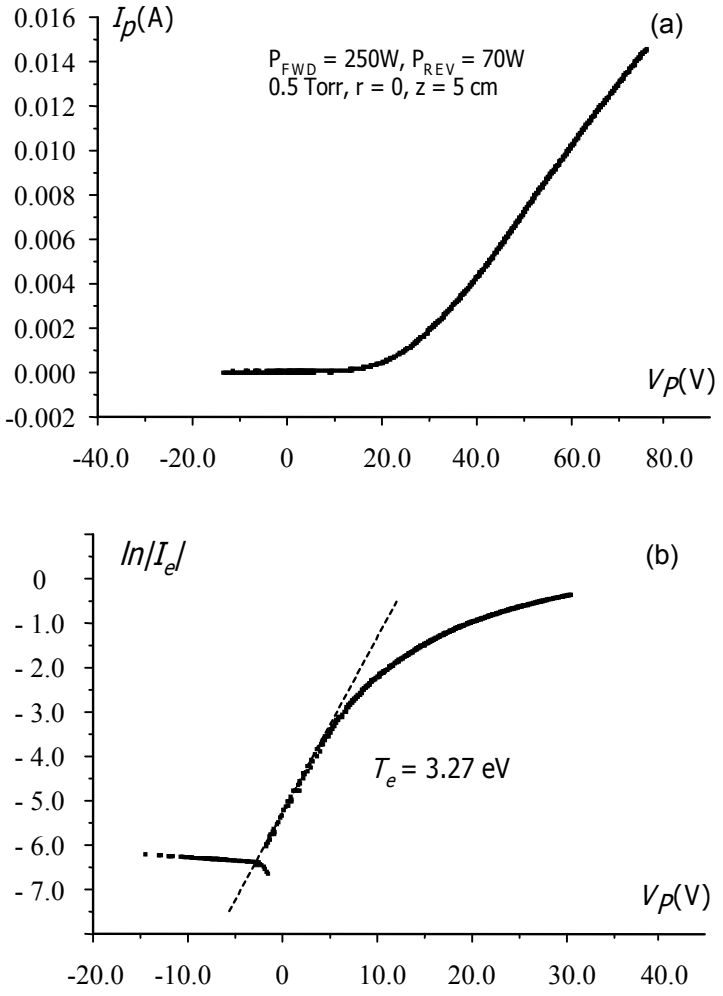

Figure 5. (a) I-V plot for the compensating Langmuir probe inside a plasma with power dissipated into the plasma (P_{FWD} - P_{REV}) of 180W. Probe tip is at the center of plasma 5 cm below the quartz plate. (b) electron temperature is extracted from ln (I_e) versus V_p.

Determination of the electron temperature

To derive the value of electron temperature and hence the plasma temperature in our quasi-neutral non-equilibrium plasma, a linear fit is conducted of the ion saturation portion of the I-V curve. The range of points chosen for the fitting is of the probe current, I_p points at large negative probe bias voltage, so that, electron current has negligible contribution. The linear fit of such portion is extrapolated to obtain the ion current, I_i. The electron current, I_e, is then obtained by subtracting out the ion current, I_i, from the plasma current, I_p.

Typically, the electron current, I_e, for any Maxwellian plasma can be expressed by[20,21]

$$I_e \propto \exp\left(-\frac{eV_p}{kT_e}\right) \qquad \ldots (3)$$

Therefore, one can find the electron temperature by fitting I_e versus V_p on a semi-log plot as shown in Figure 5(b).

Determination of the plasma density

For a quasi-neutral plasma, $n_e \approx n_i \approx n_p$, where n_e , n_i and n_p are the electron density, ion density and plasma density respectively. Once T_e is known, the plasma density can be obtained from the ion saturation current, $I_{i(sat)}$ at large negative value of probe bias voltage. In this experiment, usually at V_p larger than negative 100V, ion current is expected to be saturated. Since ions have lower mobility than electrons, $I_{i(sat)}$ experience less distortion than the electron saturation current and therefore is used to determine the plasma density, n_p, from equation (4).[20,21]

$$n_p = \frac{1}{0.6eS}\sqrt{\frac{M_i}{kT_e}} \cdot I_{i(sat)} \qquad \ldots (4)$$

where e is the charge of electron, S is the area of the exposed probe surface, M_i is the ion mass of the gaseous ion and k is the Boltzmann's constant.

RESULTS AND DISCUSSIONS

Discharge characteristics

During each discharge, the tunable vacuum capacitor was adjusted for the minimum reflected power of each plasma condition by means of the RF generator wattmeter. The data in Figure 6 are presented as functions of power dissipated into the plasma, P_{DIS}, which is the total forward power P_{FWD}, minus the reverse reflected power P_{REV}, minus resistive losses $I^2_{coil}R_{eff}$, where R_{eff} is the total resistance of the coil and surrounding peripheral and I_{coil} is the planar coil current. R_{eff} is determined from the forward power while no plasma is present. This is accomplished by powering the system under high vacuum.

The experiments were carried out at an Argon pressure between 0.05 - 2 Torr, P_{DIS} range from 10 to 250 Watts. The compensating Langmuir probe tip was fixed at the center of discharge, 5 cm below the quartz plate. The discharges show mode transition and hysteresis behavior as in Figure 6. At low P_{DIS}, both coil current and voltage gradually increased as P_{DIS} increased. This was accompanied by faint light emission from the discharge. However, at P_{DIS} around 50 Watts, a sudden drop in both coil current and voltage occurred and a dramatic increase of the light emission was observed. Such abrupt change was referred to as E-H mode transition and is also reported by Seo *et al*.,[22] Kortshagen *et al*.[23] and El-Fayoumi *et al*.[2,4] However, the transition in the present work seemed to happen at much lower plasma power than that of Seo et.al. whose transition appeared at around 280 Watts of 19 MHz RF power.

This lower plasma power transition level could be explained by writing the average energy transfer from RF field, U_{RF}, by the planar coil to the electron as[25]

$$U_{RF} = \frac{eE_P^2}{2m(\nu^2 + \omega^2)}$$

where E_P is the electric field intensity, ν is the momentum transfer collision frequency and ω is the angular frequency of the field. For a fixed value of E_P, the increase in RF frequency causes the energy transfer to be inadequate to establish H-mode. Therefore a higher RF energy or RF current is consequently needed for the transition in a higher frequency discharge as presented by the above authors.

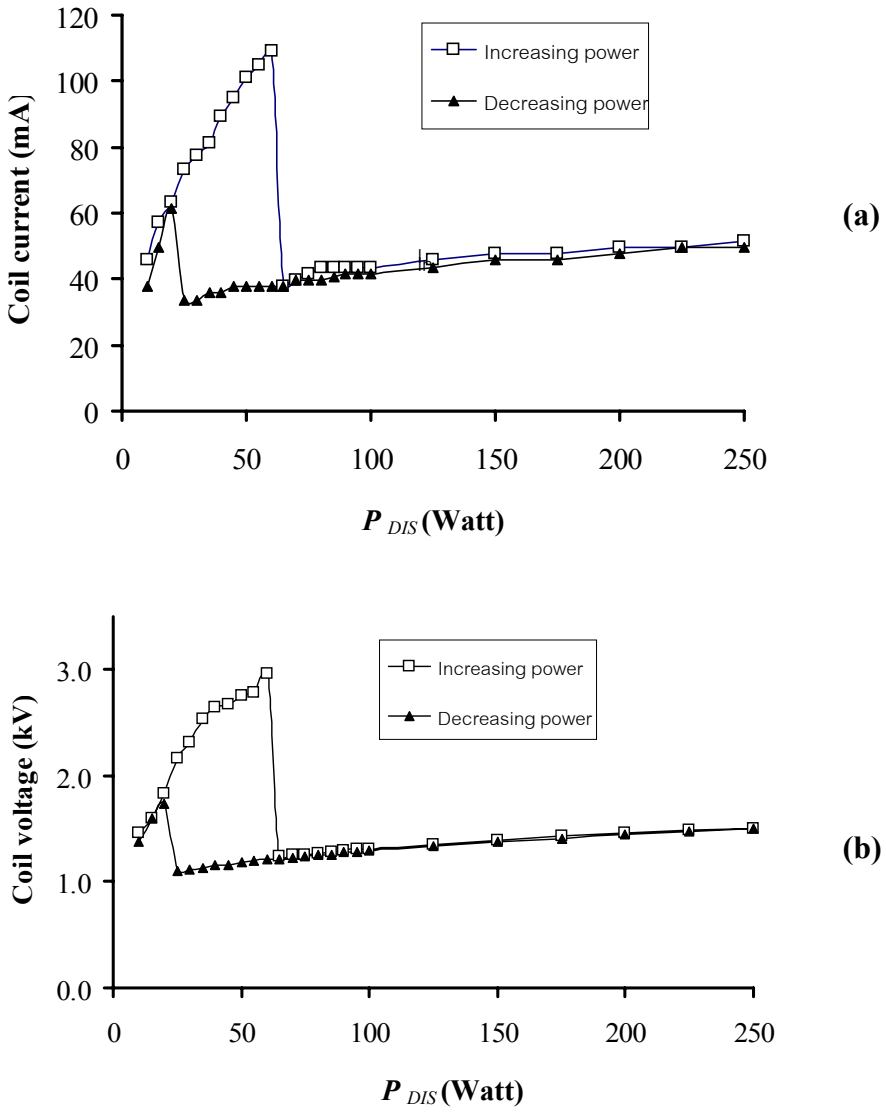

Figure 6. Planar coil current (a) and coil voltage (b) versus power dissipated into the plasma of Ar at pressure of 0.5 Torr.

Electron temperature and plasma density of the Argon TCP

Figures 7 and 8 show the variations of the plasma density and temperature at the discharge power at Ar pressure of 0.05, 0.5 and 2 Torr. In general, the variation of the electron temperature and plasma density measured using the compensated Langmuir probe is in agreement with the results reported by Hopwood *et* al[5] and Ikada *et al*.[14] The electron temperature measured for the plasma at Ar gas pressure of 0.05 Torr is slightly higher compared to that measured from 0.5 and 2.0 Torr Ar at the same P_{DIS} power. This higher electron temperature at lower pressure is expected because the number of particles per unit volume in the discharge is lower. Hence, the average kinetic energy of the electrons is higher due to longer average mean free path and lower electron-particles collision frequency.

Also, the electron temperature, T_e, appears to gradually decrease from 4 to about 2.5 eV while P_{DIS} increases from 10 to 250 Watts, in all three pressure ranges tested. This decrease in T_e may be correlated to the increase in the plasma density, n_p, where the increase in the collision frequency between electrons and the positively charged Ar ions results in the lowering of the electron temperature.

The electron temperature seems to decrease with increasing power. However, at around 50 Watts, where E to H mode transition occurs, the electron temperature jump phenomena does not occur. A quite consistent result is obtained in the 2 Torr Ar discharge where not much fluctuation is seen with the increase in power. This rather smooth transition in electron temperature is also consistent with the RF-ICP work by Schwabedissen *et al*.[7]

Nevertheless, in Figure 8, the plasma density shows an abrupt increase at the E to H mode transition. Plasma density immediately after the transition into the H mode was determined to be on the order of 10^{11} cm^{-3}. The density of the plasma was observed to increase by almost one order of magnitude from E-mode to H-mode. This indicates a greater degree of ionization in the H mode discharge. In addition to this, it was observed that the ions in the H mode plasma were more concentrated around the diameter of the planar coil as compared to the E-mode plasma, where the ions are more diffusive. An increase in the discharge power in the H-mode results in an almost linear increase in the ion, and hence the plasma, density, as shown in Figure 8. These trends are the same as those reported in previous studies.[5,7,14] However, the maximum plasma density produced, at comparable Ar pressure, in this present work (1.48×10^{12} cm^{-3}) is slightly higher than those previously reported which were about 6×10^{11} cm^{-3}. The maximum plasma density that can be measured without destroying (melting) the probe tip, in this work, is about 1.6×10^{12} cm^{-3}.

Figure 9 shows the variation in plasma potential of the discharge. It is noticed that the plasma potential in the experiments is always positive. This should come from the fact that both ions and electrons tend to diffuse from the plasma where a higher density exists. However, electrons have much higher mobility, so a slight positive space charge develops in the volume.

The variation trend of the plasma potential to the P_{DIS} very much follows that of the electron temperature. At low power, plasma potential shows a slight drop to around 50 Watts where mode transition occurs. After that, a rather constant plasma potential is obtained. This is also in agreement with the works by Schwabedissen *et al*.[7] and Seo *et al*.[22]

It is important to further note that the plasma potential of TCP is very much governed by the electrons. The evidence is shown in the increase of plasma potential with decreasing Ar pressure. As already discussed, the increase of electron temperature with decreasing pressure is caused by the lower rate of electron-particle collisions. This relates to the increase of TCP plasma potential because, in such lower collision rate, the rate of electrons escaping out from the plasma boundary to the chamber wall increases. Hence a loss of negative charge leads to higher plasma potential.

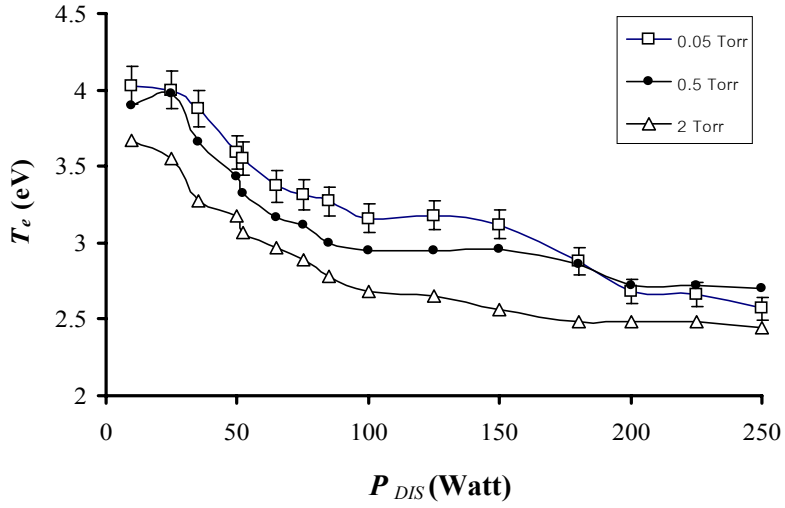

Figure 7. A comparative plot of electron temperature (T_e) versus power dissipated into the plasma of Ar at pressure of 0.05, 0.5 and 2.0 Torr.

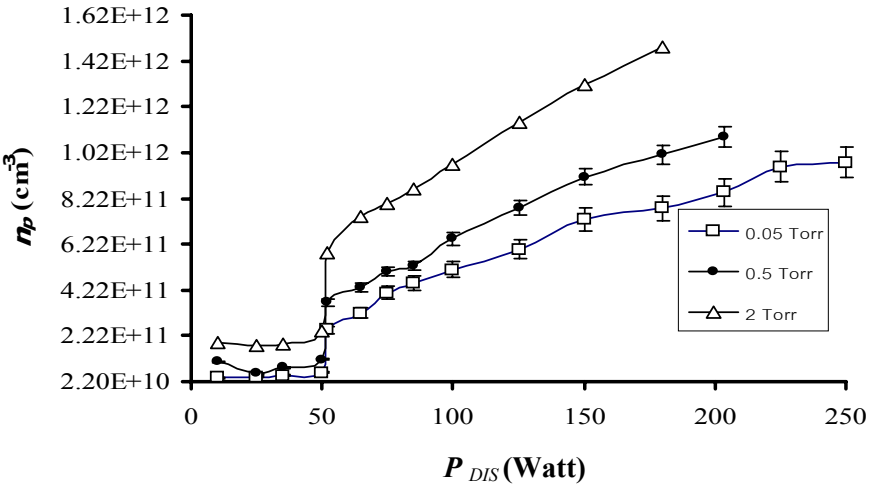

Figure 8. A comparative plot of plasma density (n_p) versus power dissipated into the plasma of Ar at pressure of 0.05, 0.5 and 2.0 Torr.

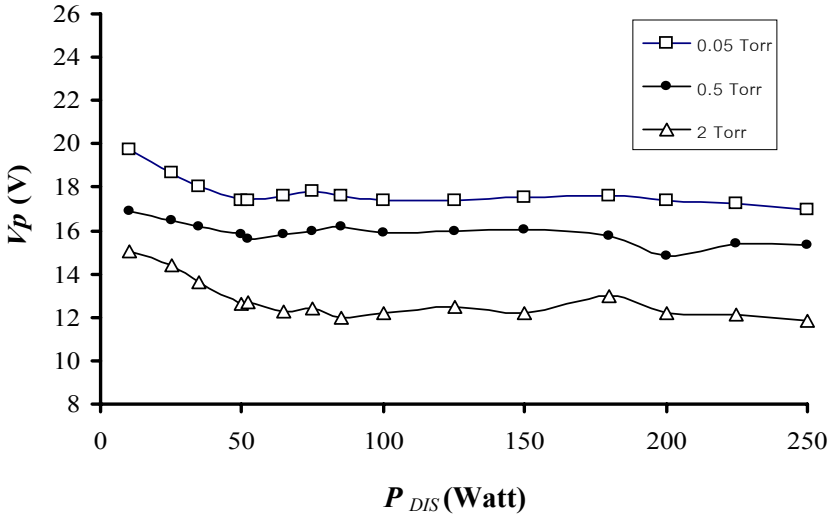

Figure 9. Variation of plasma potential with the RF power dissipated into the plasma at different Ar pressures.

CONCLUSIONS

The design and construction of a TCP system are reported. The utilization of the compensated Langmuir probe technique to measure plasma parameters, such as electron temperature and ion density in the TCP system, are discussed and compared to those reported by other groups. A significant increase in the plasma density during E to H mode transition of the TCP plasma is demonstrated by measurements obtained from the probe. Electron temperature during the TCP discharge is found to be from 2.5 - 4 eV. Plasma density in the E mode is found to be in the range of 2.2×10^{10} to 2.2×10^{11} cm^{-3}. In the H-mode the ion density was found to be in the range from 2.4×10^{11} to 1.48×10^{12} cm^{-3}. The plasma potential of the TCP is between 12 to 20 V. However, neither an abrupt change in the electron temperature nor the plasma potential is observed during E to H mode transition.

ACKNOWLEDGMENTS

The author would like to thank Prof. C.S. Wong for his initiation of the project as well as his expert suggestions. The appreciation as well goes to his group: Dr. C.O. Hoong and Mr. N.K. Hooi. Thanks also to Dr. M. Nisao for his assistance in measurement and discussion.

This project is partly support by the Office of the National Research Council of Thailand (Grant No. 0006/4222).

REFERENCES

1. Godyak, V. A., Piejak R. B. and Alexandrovich, B. M. (1994) "Electrical characteristics and electron heating mechanism of an inductively coupled argon discharge" *Plasma Sources Sci. Technol.* **2**, 169.
2. Kushner, M. J., Collison, W. Z. and Grapperhaus, M. J. (1996) "A three-dimensional model for inductively coupled plasma etching reactors: azimuthal symmetry, coil properties and comparison to experiments" *J. App. Phys*. **80(3)**, 1337.

3. Seo, S. H., Chung. C. W. and Chang, H. Y. (2000) "Review of heating mechanism in inductively couple plasma" *Surface & Coating Technol*. **131**, 1.
4. Hopwood, J. (1992) "Review of inductively coupled plasmas for plasma processing" *Plasma Sources Sci. Technol*. **2**, 109.
5. Hopwood, J., Guarnieri, C. R., Whitehair, S. J. and Cuomo, J. J. (1993) "Langmuir probe measurements of a radio frequency induction plasma" *J. Vac. Sci. Technol*. **A 11(1)**, 152.
6. Barnes, M. S., Forster J. C. and Keller, J. H. (1993) "Electron energy distribution function measurements in a planar inductive oxygen radio frequency glow discharge" *Appl. Phys. Lett*. **62**, 2622.
7. Schwabedissen, A., Benck, E. C. and Roberts, J. R. (1998) "Comparison of electron density measurements in planar inductively coupled plasmas by means of the plasma oscillation method and Langmuir probes" *Plasma Sources Sci. Technol*. **7**, 119.
8. Beale, D. F., Wendt, A. E. and Mahoney, L. J. (1994) "Spatially resolved optical emission for characterization of a planar RF inductively coupled discharge" *J. Vac. Sci. Technol*. **A12**, 2775.
9. Hori, T., Bowden, M. D., Uchino, K., Muraoka, K. and Maeda, M. (1996) "Measurements of electron temperature, electron density and neutral density in a radio-frequency inductively coupled plasma" *J. Vac. Sci. Technol.* **A14**, 144.
10. Humphreys, D. A. and Taylor, P. L. (2000) "Measurement of plasma electron temperature and effective charge during tokamak disruptions" *Phys. Plasmas* **7(10)**, 4052.
11. Huddlestone R. H. and Stanley, L. L. (1965) Plasma Diagnostic Techniques, Academic Press.
12. Godyak, V. A., Piejak R. B. and Alexandrovich, B. M. (1993) "Probe diagnostics of non-Maxwellian plasmas" *J. Appl. Phys.* **73(8)**, 3657.
13. Schwabedissen, A., Benck, E. C. and Roberts, J. R. (1997) "Langmuir probe measurements in an inductively coupled plasma source" *Phys. Rev. E.* **55(3)**, 3450.
14. Ikada, R., Nishimura, G., Kato, K. and Iizuka, S. (2004) "Production of high density and low electron-temperature plasma by a modified grid-biasing method using inductively coupled RF discharge" *Thin Solid Films* **457**, 55.
15. Chatterton, P. A., Rees, J. A., Wu, W. L. and Al-Assadi, K. A. (1991) "A self-compensating Languir probe for use in rf (13.56 MHz) plasma systems" *Vacuum* **42 (7)**, 489.
16. Bardos, L., Barankova, H., Gustavsson, L.E. and Teer, D. G. (2004) "New microwave and hallow cathode hybrid plasma sources" *Surface & Coating Technol.* **177-178**, 651.
17. Kulisch, W., Colpo, P., Rossi, F., Shtansky, D.V. and Levashov (2004) "Characterization of a hybrid PVD/PACVD system for the deposition TiC/Cao nanocomposite films by OES and probe measurements" *Surface & Coating Technol*. (in press).
18. Dhayal, M. and Bradley, J. W. (2004) "Time-resolved electric probe measurements in pulsed-plasma polymerisation of acrylic acid" *Surface & Coating Technol*. (in press).
19. Keller, J. H., Forster J. C. and Barnes, M. S. (1993) "Novel radio-frequency induction plasma processing techniques" *J. Vac. Sci. Technol.* **A11**, 2487.
20. Bittencourt, J. A. (1986), Fundamentals of Plasma Physics, *Pergamon Press*, pp 300-303.
21. Roth, J. R. (1995) *Industrial Plasma Engineering* Vol. 1., Institute of Physics Publishing, 320-325.
22. Seo, S. H., Hong, J. I., Bai, K. H. and Chang, H. Y. (1999) "On the heating mode transition in-high frequency inductively coupled argon discharge" *Phys. Plasma* **6 (2)**, 614.
23. Kortshagen, U., Gibson, N. D. and Lawler, J. D. (1996) "On the E-H mode transition in RF inductive discharges" *J. Phys. D: Appl. Phys*. **29**, 1224.
24. El-Fayoumi, I. M., Jones, I. R. and Turner, M. M. (1998) "Hysteresis in the E to H mode transition in a planar coil, inductively coupled rf argon" *J. Phys. D: Appl. Phys.* **31**, 3082.

25. Ferreira, C. M., Alves, L. L. Pinheiro, M. and Sa, A. B. (1991) "Modeling of low-pressure microwave discharges in Ar, He, and O2: similarity laws for the maintenance field and mean power transfer" IEEE Trans. *Plasma Sci.* **19(2)**, 229.

Received: October 6, 2004
Accepted: November 19, 2004